Highlights

A note on the spheroidal modes vibration of an elastic sphere in linear viscoelastic fluid

A. El Baroudi

- Exact theory for predicting spheroidal vibration of a sphere in a compressible viscoelastic fluids, is proposed.

- Complex eigenfrequency equation is established in order to quantitatively analyze the sphere vibration behavior.

- Complex eigenfrequency equation reveals a very good agreement with those in the literature in some particular cases.

- Obtained results are fundamental and can serve as benchmark solution in design of liquid sensors.

A note on the spheroidal modes vibration of an elastic sphere in linear viscoelastic fluid[★,★★]

Sir A. El Baroudi[a,*,1] (Researcher)

[a]*LAMPA, Arts et Metiers Institute of Technology, 2 bd du Ronceray, 49035 Angers, France*

ARTICLE INFO

ABSTRACT

Vibration characteristics of elastic nanostructures embedded in fluid medium have been used for biological and mechanical sensing, and also to investigate the materials mechanical properties. An analytical approach based on the exact theory has been developed in this paper, to establish a new accurate and simple generalized frequency equation to predict spheroidal vibration of an elastic nanosphere, in a compressible viscoelastic fluid using linear Maxwell fluid model. To demonstrate the accuracy of the present approach, a comparison is made with the published theoretical results in the literature in some particular cases, which shows a very good agreement. Thus, the obtained frequency equation can be very useful to interpret the experimental measurements of vibrational dynamics of nanospheres and can serve as benchmark solution in design of liquid sensors.

1. Introduction

During recent years, owing to various applications, especially in designing biological and mechanical sensors, and in characterizing material properties, vibration analysis of embedded nanoparticles in fluid medium has attracted significant attention [1, 2, 3, 4, 5, 6]. The damping level present in these applications can be defined by its quality factor. A high quality factor that describes low damping is desirable for better detection sensitivity. Consequently, it is of interest to understand the damping phenomenon due to transfer of energy or energy dissipation to the surrounding medium. In addition, incited by the idea to destroy biological nanoparticles such as viruses using resonance concept of an ultrasonic wave, the elastic spheres models have also been used to study the vibration characteristics of viruses in different media. [7, 8, 9, 10, 11].

The damping mechanism and resonant frequencies of nanostructures with different shapes have been measured by a many experimental techniques [5, 12, 13]. From the modeling perspective of the vibration characteristics of these nanostructure, vibrations of elastic structures are classical problems in continuum mechanics. For example, Lamb [14] proposed a theoretical aspect to investigate the spheroidal modes of a dry elastic sphere. In spheroidal modes, the volume or shape of the sphere subjected to vibration is not constant. In addition, there are a number of works that have considered the vibration modes of elastic structures with different geometries [6, 9, 15, 16, 17].

Low frequency inelastic Raman scattering and far-infrared spectroscopy are very interesting to study the geometry and the elastic properties of nanoparticles. It was shown that the vibration of spherical nanoparticles which are visible by Raman scattering are spheroidal modes: breathing and quadrupolar [18, 19, 20, 21, 22]. By far infrared spectroscopy, only the dipolar spheroidal mode can be observed. Furthermore, investigations on the dynamical properties of viruses through inelastic Brillouin light-scattering [23] highlight also spheroidal modes: breathing and quadrupolar. The dipolar spheroidal mode is the only to directly interact with microwaves [24, 25]. However the free sphere model used to interpret the experimental results is an approximation of the actual environmental conditions of nanoparticles.

A recent theoretical study based on the purely radial vibration mode (Breathing mode) of a gold nanosphere was developed to predict a viscoelastic response in water-glycerol mixtures [26]. This study demonstrates that an increase in glycerol mass fraction, the non-monotonic variations of quality factor are displayed and not captured by Newtonian fluid model. However a viscoelastic fluid model highlights the non-monotonic behavior. Nevertheless, the spheroidal vibrations modeling (quadrupolar and dipolar mode) is still lacking. Different vibration modes of nanosphers have been experimentally observed [23, 24, 25], and hence it is very important to establish a generalized eigenfrequency equation based on the exact theory in order to characterize the general vibration behavior other than the breathing mode [26, 27]. In this paper, a more general theory for predicting the spheroidal vibrations of an elastic sphere is proposed, in a compressible viscoelastic fluid using the Maxwell model.

2. Compressible viscoelastic fluid

We begin by briefly reviewing the conservation equations for a general fluid. Throughout, we assume that the flow exhibits small-amplitude acoustic oscillations so that all nonlinear convective terms can be neglected. Hence, the velocity field, $\mathbf{v}$, is governed by the linearized Navier-Stokes equation for compressible flows

$$\rho_f \partial_t \mathbf{v} = \nabla \cdot \mathbf{T}^{(f)} \tag{1}$$

*Corresponding author

✉ adil.elbaroudi@ensam.eu (A.E. Baroudi)
🌐 https://elbaroudi.wordpress.com/ (A.E. Baroudi)
ORCID(s): 0000-0002-6860-4877 (A.E. Baroudi)

where ρ_f is the fluid density at equilibrium. The total stress in a compressible fluid, $\mathbf{T}^{(f)}$, can be written as

$$\mathbf{T}^{(f)} = -p\mathbf{I} + \boldsymbol{\sigma} + \boldsymbol{\tau} \tag{2}$$

where p is the thermodynamic pressure and $\mathbf{I}$ is the identity tensor. For a compressible Newtonian fluid, $\boldsymbol{\sigma}$ and $\boldsymbol{\tau}$ are the compressional and shear contributions to the deviatoric stress tensor, respectively, and which are related to the deformation by the following constitutive equations

$$\boldsymbol{\sigma} = \kappa \left(\mathrm{tr}\mathbf{D} \right) \mathbf{I} \quad , \quad \boldsymbol{\tau} = 2\eta \left(\mathbf{D} - \frac{\mathrm{tr}\mathbf{D}}{3} \mathbf{I} \right) \tag{3}$$

where κ and η are respectively, the bulk and shear viscosities of the fluid, and $\mathbf{D} = \left[\nabla\mathbf{v} + (\nabla\mathbf{v})^T \right] / 2$ is the strain rate tensor. In order to describe the fluid viscoelasticity, the linear Maxwell model is employed. In this case, the relation between force and deformation can be written as [27]

$$\begin{aligned} \delta_c \partial_t \boldsymbol{\sigma} + \boldsymbol{\sigma} &= \kappa \left(\mathrm{tr}\mathbf{D} \right) \mathbf{I} \\ \delta_s \partial_t \boldsymbol{\tau} + \boldsymbol{\tau} &= 2\eta \left(\mathbf{D} - \frac{\mathrm{tr}\mathbf{D}}{3} \mathbf{I} \right) \end{aligned} \tag{4}$$

where δ_s and δ_c are respectively, the shear and compressional relaxation time. In a Maxwell fluid, the viscoelastic behavior is modeled as a purely viscous damper and a purely elastic spring connected in series. Note that more details about tensor representations of constitutive equations for viscoelastic fluids can be found in [28, 29].

The linearized Navier-Stokes equation (1) must be completed by the continuity equation. Because the small-amplitude acoustic oscillations are considered, the continuity equation for a compressible fluid is given by

$$\partial_t \rho + \rho_f \nabla \cdot \mathbf{v} = 0 \tag{5}$$

where ρ represents the density fluctuation. In addition, the equation of state relating the density fluctuation to the thermodynamic pressure is given by $p = c_f^2 \rho$, where c_f is the speed of sound in the fluid [30]. In other words, for small-amplitude acoustic waves, one can assume that a small change in fluid density induces small changes in pressure by fast adiabatic process.

2.1. Velocity potential formulation

Equation (1) can be transformed into simple scalar equations by introducing the velocity potentials. Any sufficiently smooth vector field can be written as the sum of the gradient of a scalar field and the curl of a vector field. This is called the Helmholtz representation [31]. For the velocity field considered here, that representation is

$$\mathbf{v} = \mathbf{v}_p + \mathbf{v}_s \tag{6}$$

where each component has specific properties : (*i*) Potential component with curl-free component, i.e. $\nabla \times \mathbf{v}_p = \mathbf{0}$, so it stems from a scalar potential ϕ : $\mathbf{v}_p = \nabla\phi$. This component describes the compressible part of the velocity field. (*ii*) Solenoidal component with divergence-free component,

i.e. $\nabla \cdot \mathbf{v}_s = 0$, so it stems from vector potential $\boldsymbol{\psi}$: $\mathbf{v}_s = \nabla \times (r\psi\mathbf{e}_r)$. This component describes the incompressible part of the velocity field. Substitution of Eq. (6) into Eq. (1) and taking into account Eq. (4), yields the acoustic pressure in terms of the velocity potential

$$p = \left[\kappa \left(1 + \delta_c \partial_t \right)^{-1} + \frac{4\eta}{3} \left(1 + \delta_s \partial_t \right)^{-1} \right] \nabla^2 \phi - \rho_f \partial_t \phi \tag{7}$$

In the same way, one can easily demonstrate that the potential ψ satisfies the following equation

$$\rho_f \left(1 + \delta_s \partial_t \right) \partial_t \psi = \eta \nabla^2 \psi \tag{8}$$

Concerning the potential ϕ, combination of Eq. (5), equation of state and Eq. (7) yields

$$\partial_{tt}\phi = \left\{ c_f^2 + \left[\kappa \left(1 + \delta_c \partial_t \right)^{-1} + \frac{4\eta}{3} \left(1 + \delta_s \partial_t \right)^{-1} \right] \frac{\partial_t}{\rho_f} \right\} \nabla^2 \phi \tag{9}$$

The determination of the potentials ϕ and ψ requires the resolution of the Helmholtz equation (9) and the diffusion equation (8), respectively. In this work time-harmonic dependence $e^{j\omega t}$ is assumed. Therefore, using previously developed techniques [31], the potentials ϕ and ψ take the following forms

$$\phi = \sum_{n=0}^{\infty} \sum_{m=-n}^{n} \sqrt{\frac{\pi}{2k_c r}} \left[A_1 J_{n+\frac{1}{2}} \left(k_c r \right) + B_1 Y_{n+\frac{1}{2}} \left(k_c r \right) \right]$$
$$\times \sin(m\varphi) P_n^m(\cos\theta)$$

$$\psi = \sum_{n=0}^{\infty} \sum_{m=-n}^{n} \sqrt{\frac{\pi}{2k_s r}} \left[A_2 I_{n+\frac{1}{2}} \left(k_s r \right) + B_2 K_{n+\frac{1}{2}} \left(k_s r \right) \right]$$
$$\times \cos(m\varphi) P_n^m(\cos\theta)$$

where

$$k_c = \cfrac{\omega}{c_f \sqrt{1 + \cfrac{j\omega}{\rho_f c_f^2} \left[\cfrac{\kappa}{1 + j\omega\delta_c} + \cfrac{4\eta}{3\left(1 + j\omega\delta_s\right)} \right]}}$$

$$k_s = \sqrt{\frac{j\omega\rho_f}{\eta} \left(1 + j\omega\delta_s \right)} \tag{10}$$

and A_1, B_1, A_2 and B_2 are arbitrary constants, $J_{n+\frac{1}{2}}$ and $Y_{n+\frac{1}{2}}$ are Bessel functions of the first and second kind and $I_{n+\frac{1}{2}}$ and $K_{n+\frac{1}{2}}$ are modified Bessel functions of the first and second kind, $P_n^m(\cos\theta)$ are associated Legendre polynomials. In addition, the time factor $e^{j\omega t}$ is omitted for simplicity. Hence, introducing the parameter $\eta^* = \eta / \left(1 + j\omega\delta_s \right)$, the components of the velocity field and stress tensor that will be further used in boundary conditions are given by

$$\begin{aligned} v_r &= \frac{\partial\phi}{\partial r} + \frac{\partial^2(r\psi)}{\partial r^2} - k_s^2 r\psi \\ v_\theta &= \frac{1}{r}\frac{\partial}{\partial\theta} \left[\phi + \frac{\partial(r\psi)}{\partial r} \right] \end{aligned} \tag{11}$$

$$\frac{T_{rr}^{(f)}}{2\eta^*} = \frac{\partial^2\phi}{\partial r^2} + \left(\frac{k_s^2}{2} + k_c^2\right)\phi + \frac{\partial}{\partial r}\left[\frac{\partial^2(r\psi)}{\partial r^2} - k_s^2 r\psi\right]$$

$$\frac{T_{r\theta}^{(f)}}{2\eta^*} = \frac{\partial}{\partial\theta}\left\{\frac{1}{r^2}\left(r\frac{\partial\phi}{\partial r} - \phi\right) + \frac{\partial}{\partial r}\left[\frac{1}{r}\frac{\partial(r\psi)}{\partial r}\right] - \frac{k_s^2\psi}{2}\right\}$$

(12)

3. Elastic sphere

In this section, the constitutive equation Eq. (4) for a compressible viscoelastic fluid is used to study the fluid-structure interaction of a submerged elastic sphere. The aim here is to demonstrate how mode shape affects the resulting flow dynamics. This solution also finds direct application in practice, because these particles are often measured using ultrafast laser spectroscopy to probe their dynamics [5, 32, 33, 34, 35]. Therefore, it has been established that nanometer-sized solid particles obey the continuum hypothesis [6, 12, 36, 37] with their dynamics being governed by Navier's equation

$$\partial_{tt}\mathbf{u} = C_s^2\left(\nabla^2\mathbf{u} - \nabla\nabla\cdot\mathbf{u}\right) + C_c^2\nabla\nabla\cdot\mathbf{u}$$

(13)

where $\mathbf{u}$ is the displacement field and, $C_c = \sqrt{(\lambda + 2\mu)/\rho_s}$ and $C_s = \sqrt{\mu/\rho_s}$ are the propagation velocities of compressional and shear waves in the elastic sphere, respectively. ρ_s is the solid density and λ and μ are the Lamé parameters. As before, it is assumed that the particle undergoes small-amplitude oscillations, and thus the usual assumption of linear elasticity is applicable. In a similar manner that fluid velocity potential, the Navier's equation (13) can be easily transformed into the following form in terms of the scalar potentials

$$C_c^2\nabla^2\Phi - \partial_{tt}\Phi = 0, \quad C_s^2\nabla^2\Psi - \partial_{tt}\Psi = 0$$

(14)

The solution of Eq. (14) can, of course, be expressed in terms of Bessel functions

$$\Phi = \sum_{n=0}^{\infty}\sum_{m=-n}^{n}\sqrt{\frac{\pi}{2K_c r}}A_3 J_{n+\frac{1}{2}}\left(K_c r\right)\sin(m\varphi)P_n^m(\cos\theta)$$

$$\Psi = \sum_{n=0}^{\infty}\sum_{m=-n}^{n}\sqrt{\frac{\pi}{2K_s r}}B_3 J_{n+\frac{1}{2}}\left(K_s r\right)\cos(m\varphi)P_n^m(\cos\theta)$$

where A_3 and B_3 are arbitrary constants and $K_c = \omega/C_c$ and $K_s = \omega/C_s$ are the compressional and shear wavenumbers. Also, according to the generalized Hooke's law, the radial stress in terms of displacement potential, that will further used in boundary conditions is expressed

$$\frac{T_{rr}^{(s)}}{2\mu} = \frac{\partial^2\Phi}{\partial r^2} - \frac{\lambda K_c^2}{2\mu}\Phi + \frac{\partial}{\partial r}\left[\frac{\partial^2(r\Psi)}{\partial r^2} + K_s^2 r\Psi\right]$$

In addition, to obtain the displacement components and tangential stress, the velocity potentials (ϕ, ψ) must be replaced by the displacement potentials (Φ, Ψ) in Eq. (11), and viscosity η^* by shear modulus μ in Eq. (12).

4. Sphere-fluid interaction

The vibration frequencies of the coupled system shall be obtained by application of the appropriate boundary conditions. Therefore, the following relations are suitable : (i) Flux continuity that describes mass conservation and equilibrium of the normal forces at the sphere-fluid interface

$$v_r = \frac{\partial u_r}{\partial t}, \quad v_\theta = \frac{\partial u_\theta}{\partial t}, \quad T_{rr}^{(f)} = T_{rr}^{(s)}, \quad T_{r\theta}^{(f)} = T_{r\theta}^{(s)}$$

(15)

(ii) The nonslip boundary condition for the outside surface of viscoelastic fluid is assumed

$$v_r = 0, \quad v_\theta = 0$$

(16)

Eqs. (15)-(16) give for each mode number n the following equation of the spheroidal vibrations (or vibrations of second-class [14])

$$[\mathbf{S}]\{\mathbf{y}\} = \mathbf{0}, \quad \{\mathbf{y}\} = \left\{A_1, B_1, A_2, B_2, A_3, B_3\right\}^T$$

(17)

In spheroidal vibrations, the volume of the sphere subjected to vibration is not constant and the displacement vector must be defined by two independent components u_r and u_θ. In spheroidal modes, $n = 0$ corresponds to purely radial vibration mode, the so-called breathing, $n = 2$ occurs at frequencies lower than $n = 0$ and is characterized by an oscillation of the field between the forms of an oblate spheroid and a spheroid elongated at the poles (oblate-prolate). Furthermore, $\mathbf{S}$ is a 6×6 matrix whose elements are designated as S_{ij} and are given in Appendix A. For a non-trivial solution, the determinant of the matrix $\mathbf{S}$ must be equal to zero, which leads to the following eigenfrequency equation

$$\det\mathbf{S} = 0$$

(18)

where

$$\mathbf{S} = \begin{pmatrix} \dfrac{S_{11}}{\sqrt{k_c}} & \dfrac{S_{12}}{\sqrt{k_c}} & \dfrac{S_{13}}{\sqrt{k_s}} & \dfrac{S_{14}}{\sqrt{k_s}} & -j\omega\dfrac{S_{15}}{\sqrt{K_c}} & -j\omega\dfrac{S_{16}}{\sqrt{K_s}} \\[2mm] \dfrac{S_{21}}{\sqrt{k_c}} & \dfrac{S_{22}}{\sqrt{k_c}} & \dfrac{S_{23}}{\sqrt{k_s}} & \dfrac{S_{24}}{\sqrt{k_s}} & -j\omega\dfrac{S_{25}}{\sqrt{K_c}} & -j\omega\dfrac{S_{26}}{\sqrt{K_s}} \\[2mm] \dfrac{\eta^* S_{31}}{\sqrt{k_c}} & \dfrac{\eta^* S_{32}}{\sqrt{k_c}} & \dfrac{\eta^* S_{33}}{\sqrt{k_s}} & \dfrac{\eta^* S_{34}}{\sqrt{k_s}} & -\dfrac{\mu S_{35}}{\sqrt{K_c}} & -\dfrac{\mu S_{36}}{\sqrt{K_s}} \\[2mm] \dfrac{\eta^* S_{41}}{\sqrt{k_c}} & \dfrac{\eta^* S_{42}}{\sqrt{k_c}} & \dfrac{\eta^* S_{43}}{\sqrt{k_s}} & \dfrac{\eta^* S_{44}}{\sqrt{k_s}} & -\dfrac{\mu S_{45}}{\sqrt{K_c}} & -\dfrac{\mu S_{46}}{\sqrt{K_s}} \\[2mm] \dfrac{S_{51}}{\sqrt{k_c}} & \dfrac{S_{52}}{\sqrt{k_c}} & \dfrac{S_{53}}{\sqrt{k_s}} & \dfrac{S_{54}}{\sqrt{k_s}} & 0 & 0 \\[2mm] \dfrac{S_{61}}{\sqrt{k_c}} & \dfrac{S_{62}}{\sqrt{k_c}} & \dfrac{S_{63}}{\sqrt{k_s}} & \dfrac{S_{64}}{\sqrt{k_s}} & 0 & 0 \end{pmatrix}$$

Eigenfrequency equation (18) constitutes an implicit transcendental function of n and ω. The roots ω may be computed for a fixed n. It is interesting to note that this eigenfrequency equation is independent of the values of m due to the spherical symmetry. It should be pointed out that in the eigenfrequency (18), dipolar mode corresponds to $n = 1$ and quadrupolar mode to $n = 2$.

4.1. Some particular cases

For the general analytical approach developed in this paper for spheroidal modes of vibration, it is very important to check its accuracy in some particular cases. In the case of radial vibration mode, it is easy to show that the equation (18) takes the following simple form

$$K_c^2 a^2 \left[\frac{\rho_f}{\rho_s \left(1 - jk_c a\right)} + \left(\frac{K_c a}{\tan\left(K_c a\right)} - 1 \right)^{-1} \right]$$
$$+ \frac{4j\eta K_c}{\rho_s C_c \left(1 - j\omega\delta_s\right)} + 4 \left(\frac{C_s}{C_c} \right)^2 = 0 \quad (19)$$

Thus, when compressional relaxation time is neglected $\left(\delta_c = 0\right)$, the equation (19) becomes

$$K_c^2 a^2 \left[\frac{\rho_f}{\rho_s \left(1 - jk_c^* a\right)} + \left(\frac{K_c a}{\tan\left(K_c a\right)} - 1 \right)^{-1} \right]$$
$$+ \frac{4j\eta K_c}{\rho_s C_c \left(1 - j\omega\delta_s\right)} + 4 \left(\frac{C_s}{C_c} \right)^2 = 0 \quad (20)$$

which was previously obtained by Galstyan *et al.* [26] and

$$k_c^* = k_c \left(\delta_c = 0\right) = \frac{\omega}{c_f \sqrt{1 - \frac{j\omega}{\rho_f c_f^2} \left[\kappa + \frac{4\eta}{3\left(1 - j\omega\delta_s\right)} \right]}}$$

A comprehensive review of radial mode of a vibrating sphere in Newtonian and linear Maxwell fluids can be found in [26, 27].

5. Comparison studies

For the general analytical approach developed in this paper, it is very important to check its accuracy and numerical robustness in some particular cases. Firstly, a comparison study is performed for a first breathing mode of a sphere submerged in a compressible linear Maxwell fluid. To compare the results derived from the equation (19) (or Eq. (18) for $n = 0$) with other theoretical established results, the same dimensionless parameters that used by Chakraborty and Sader [27] are introduced

$$\mathrm{De}_s = \delta_s \omega, \ \mathrm{De}_c = \delta_c \omega, \ \xi = \frac{\omega a}{c_f}, \ \beta = \frac{\rho_f \omega a^2}{\eta}, \ \alpha = \frac{\kappa}{\eta}$$

where De is the Deborah number. Morever, the quality factor $Q = -\sqrt{\omega_r^2 + \omega_i^2} / \left(2\omega_i\right)$, and the vibration frequency $f = \omega_r / (2\pi)$ are the same as those adopted by [26, 27], where ω_r and ω_i are, respectively, the real and imaginary parts of the angular frequency. Figure 1 shows the quality factor versus normalized frequency β for various Deborah numbers De_s. Compressible and incompressible Newtonian fluids (i.e. $\mathrm{De}_s = 0$) predict that the quality factor increases monotonically with increasing β. For large values of β, a
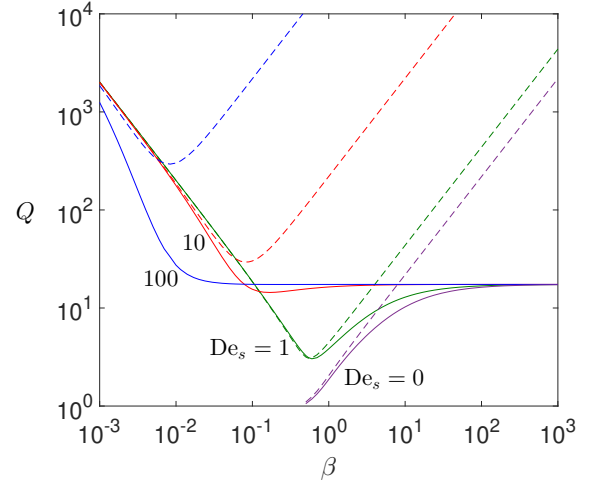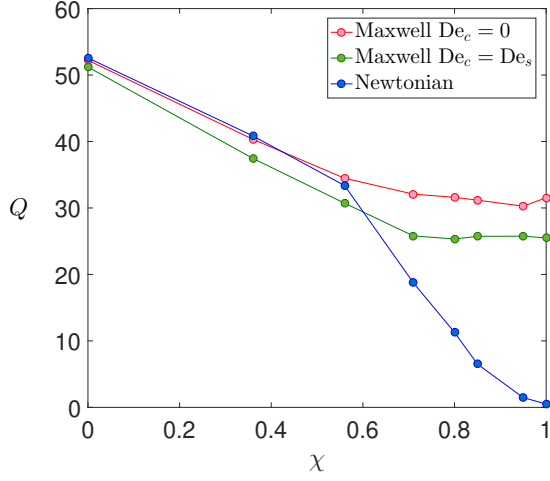

Figure 1: Quality factor of the first breathing mode of a gold nanosphere; effect of viscoelasticity and fluid compressibility. Results for radius $a = 50\,\mathrm{nm}$, Poisson's ratio $\nu = 0.44$, density ratio $\rho_s/\rho_f = 20$, viscosity ratio $\alpha = 1$, and Deborah numbers are chosen so that $\mathrm{De}_c = \mathrm{De}_s$ and normalized wavenumber $\xi = 1$. Compressible fluid (solid lines); Incompressible fluid (dashed lines).

difference between the compressible and incompressible results was observed. The behavior changes completely for non zero values of De_s. First, the elasticity results in qualitatively different behavior in the low β-regime. The quality factor increases monotonically with decreasing β. For $\beta > 1$ the scenario is different, the quality factor converges to a constant value as β increases while the incompressible solution gives a monotonically increasing quality factor. In addition, the results in the Figure 1 predicted by Eq. (19) (or Eq. (18) for $n = 0$) agree exceptionally well with those obtained by Chakraborty and Sader [27].

A second and last comparison can be drawn between the present solution and that of Galstyan *et al.* [26] in the case of the first breathing mode vibration of a sphere submerged in a Maxwell fluid without compressional relaxation process (i.e. $\mathrm{De}_c = 0$). Quality factor variation versus glycerol mass fraction in both compressible Maxwell and Newtonian fluids are investigated. Figure 2 shows that the Newtonian fluid highlights a monotonically decreasing correlation between the quality factor and glycerol mass fraction. However, the Maxwell fluids predicted a non monotonically behavior of the quality factor and glycerol mass fraction. Thus, the results in the Figure 2 agree exceptionally well with those obtained by Galstyan *et al.* [26].

6. Numerical results

Having established the accuracy through the comparison study illustrated in Figures 1 and 2, further numerical results are given in this section. The material properties used by Galstyan *et al.* [26] were taken to construct this numerical example. Thus, effect of different parameters, including sphere radius, fluid compressibility, viscosity and viscoelas-

Figure 2: Quality factor of the first breathing mode of a gold nanosphere with radius $a = 40$ (nm) as a function of glycerol mass-fraction χ.

Mode	n	$\omega_r \times 10^{11}$	$\omega_i \times 10^9$	Q	f
1	2	0.7819	2.6353	14.8439	12.4449
2	1	1.1184	2.0315	27.5317	17.8004
3	3	1.1761	3.1861	18.4649	18.7196
4	4	1.5181	3.5985	21.0997	24.1619
5	2	1.5871	3.1856	24.9152	25.2598
6	5	1.8399	3.9674	23.1927	29.2829
7	3	2.0758	4.0805	25.4412	33.0383
8	6	2.1519	4.3087	24.9770	34.2493
9	0	2.3739	3.8636	30.7254	37.7820
10	7	2.4585	4.6208	26.6071	39.1286

Table 1
Quality factor, Q and vibration frequency, f (GHz) of the gold nanosphere with 40 nm radius vibrating in water-glycerol mixture with $\chi = 0.56$.

ticity on the vibrations characteristics of the sphere are investigated.

In this work, the generalized eigenfrequency equation (18) is solved employing Mathematica software. After finding the real part ω_r and the imaginary part ω_i of the angular frequency, the frequency and quality factor can be calculated. First ten vibration frequency and quality factor of the spheroidal modes are given in Table 1 for Newtonian and Maxwell fluids with compressional relaxation process. For simplicity, Deborah numbers with $De_c = De_s$ is a good approximation for some real fluids [27]. It can be seen that the frequencies of the spheroidal vibrations corresponding to the angular mode number $1 \leq n \leq 6$ are lower than the frequency of the radial mode. Different vibration modes of nanosphers have been experimentally observed [23, 24, 25], and hence it is very important to establish an eigenfrequency equation in order to characterize the general vibration behavior other than the radial mode.

To highlight the difference between the spheroidal vibration modes and the compressional relaxation effect, the quality factor of the gold nanosphere with 40 nm radius vibrating in water ($\chi = 0$) and in water-glycerol mixture ($\chi = 0.56$ and $\chi = 0.71$) are summarized in Table 2 for Newtonian and Maxwell fluids with ($De_c = De_s$) and without ($De_c = 0$) compressional relaxation process. This Table shows a significant reduction in the quality factor due to the fluid viscosity when water is replaced by water-glycerol mixture. Table 2 also shows a sensitivity of the breathing mode to the compressional relaxation process. However, the dipolar and quadrupolar modes are not affected by this compressional relaxation process. Therefore, to reasonably predict the quality factor, the compressional relaxation effect should be considered for the breathing mode. In other words, the Maxwell fluid with compressional relaxation process proposed by Chakraborty and Sader [27] is more appropriate for breathing mode and, the Maxwell fluid without compres-

$\chi = 0.00$	$n = 0$	$n = 1$	$n = 2$
Newtonian	52.581*	91.513	25.329
Maxwell ($De_c = De_s$)	51.211	89.255	25.070
Maxwell ($De_c = 0$)	52.221*	89.233	25.338

$\chi = 0.56$	$n = 0$	$n = 1$	$n = 2$
Newtonian	33.380*	27.864	14.378
Maxwell ($De_c = De_s$)	30.725	27.531	14.444
Maxwell ($De_c = 0$)	34.474*	27.467	14.473

$\chi = 0.71$	$n = 0$	$n = 1$	$n = 2$
Newtonian	18.763*	10.008	9.175
Maxwell ($De_c = De_s$)	25.804	17.289	11.294
Maxwell ($De_c = 0$)	32.090*	16.879	12.162

Table 2
Quality factor of the gold nanosphere with 40 nm radius vibrating in water-glycerol mixture. * same value predicted by Galstyan *et al.* [26].

sional relaxation process presented by Galstyan *et al.* [26] is more suitable for dipolar and quadrupolar modes.

The quality factor of a gold nanosphere vibrating in Newtonian and Maxwell fluids with and without compressional relaxation effect as a function of angular mode number is depicted in Figure 3. On the one hand, Figure 3 shows that for the low glycerol mass fraction (i.e. small viscoelasticity effect) such as $\chi = 0.36$, and lower modes, the difference between the Maxwell and Newtonian fluids is not very significant. However, increasing angular mode number, this difference increases gradually. Moreover, for high glycerol
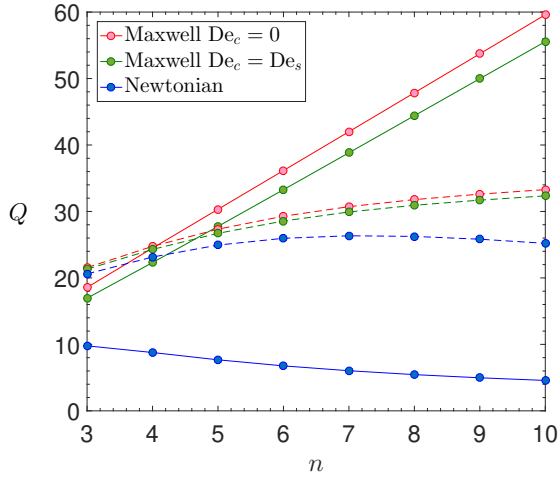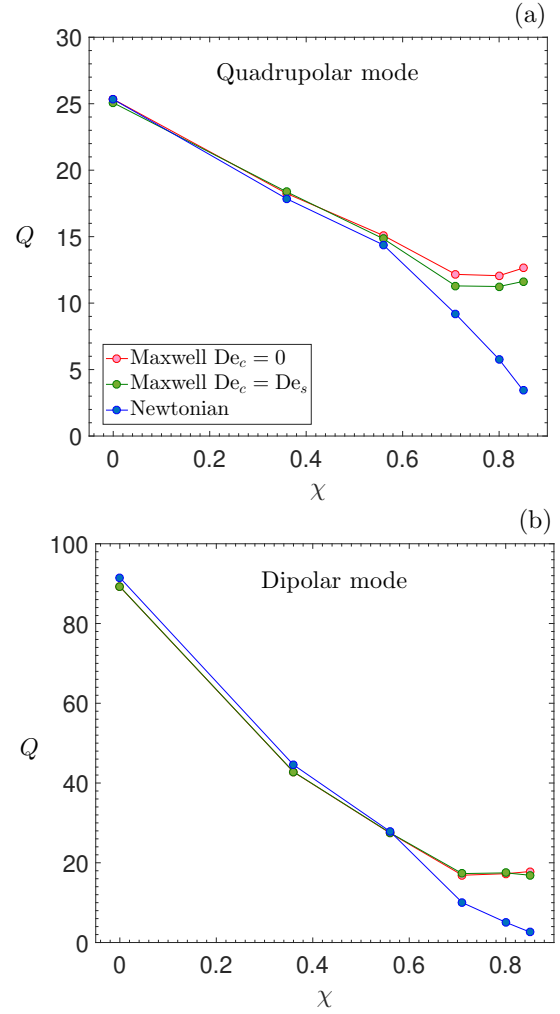
Figure 3: Quality factor of a gold nanosphere with radius $a = 40$ (nm) versus angular mode number. $\chi = 0.71$ (solid lines); $\chi = 0.36$ (dashed lines).

Figure 4: Quality factor of the first mode vibration of a gold nanosphere with radius $a = 40$ (nm) versus glycerol mass-fraction.

mass fractions (i.e. important viscoelasticity effect) such as $\chi = 0.71$, the obtained quality factor by the two fluid models is different over the entire mode range. As the angular mode number increases, the quality factor predicted using Maxwell fluids increases almost linearly, while that based on the Newtonian model monotonically decreases for increasing values of the angular mode number. On the other hand, in Figure 3 it can be seen that, for low mass fractions, the compressional relaxation effect on the higher-order modes is less significant. For high mass fractions, the quality factor strongly depends on the compressional relaxation process over the whole mode range.

The variations of the quality factor of the quadrupolar and dipolar modes of a gold nanosphere with the glycerol mass fractions in both Maxwell and Newtonian fluids are depicted in Figure 4. Increasing the glycerol mass fraction considering a Newtonian fluid, an increase in the glycerol mass fraction causes a monotonic reduction in the quality factor. However, a Maxwell fluids predicted a non-monotonic behavior due to the intrinsic viscoelastic properties of fluids.

The variations of the quality factor of the quadrupolar, dipolar and breathing modes with the elastic sphere radius for a glycerol mass fraction of $\chi = 0.56$ are illustrated in figure 5 using the Maxwell and Newtonian fluids. The predicted quality factor by the Newtonian fluid monotonically decreases with decreasing radius for all modes due to the increasing viscous dissipation effect. For the quadrupolar mode, a monotonic increase with the radius has been observed for the Maxwell fluid. Thus, the compressional relaxation effect on the quality factor is less significant. The same behavior for the dipolar mode has been highlighted. However, for the breathing mode, by varying the sphere radius, the compressional relaxation process strongly affects the quality factor because of its compressional motion behavior. A non monotonic variations of the quality factor with

the radius has been observed for the maxwell fluid without the compressional relaxation process. In addition, for the quadrupolar mode, the viscoelasticity effect occurs for radius values less than 25 nm, 35 nm for the dipolar mode and 50 nm for the breathing mode using Maxwell fluid without the compressional relaxation process.

7. Conclusion

In the this paper a generalized eigenfrequency equation has been established in order to characterize the vibration behavior of spherical particles which execute for example a dipolar, quadrupolar and breathing modes, and the following concluding remarks could be drawn :

- The obtained eigenfrequency equation (18) using the general constitutive equation (4) exhibits all the required features of a linear Maxwell fluids at low frequencies (fluid-like behavior) and at high frequencies (solid-like behavior). Therefore, this equation provides a general formalism to characterize the fluid-structure
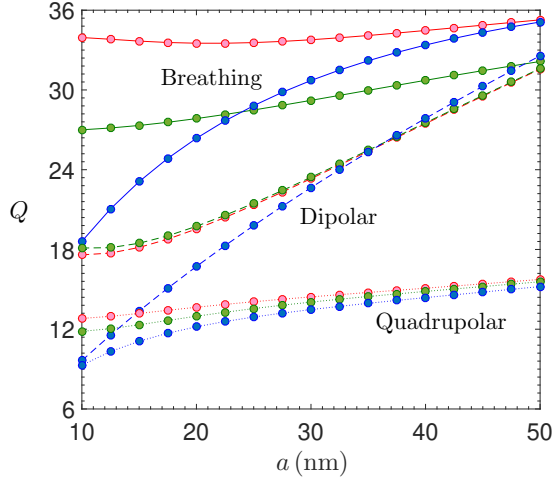
Figure 5: Quality factor of the first mode of a gold nanosphere with glycerol mass-fraction $\chi = 0.56$ versus gold nanosphere radius. Maxwell fluid $\mathrm{De}_c = 0$ (red), Maxwell fluid $\mathrm{De}_c = \mathrm{De}_s$ (green) and Newtonian fluid (blue).

For high mass fractions, the quality factor strongly depends on the compressional relaxation process over the whole mode range.

- The predicted quality factor by the Newtonian fluid monotonically decreases with decreasing radius for all modes due to the increasing viscous dissipation effect. For the quadrupolar mode, a monotonic increase with the radius has been observed for the Maxwell fluid. Thus, the compressional relaxation effect on the quality factor is less significant. The same behavior for the dipolar mode has been highlighted. However, for the breathing mode, by varying the sphere radius, the compressional relaxation process strongly affects the quality factor because of its compressional motion behavior. A non monotonic variations of the quality factor with the radius has been observed for the Maxwell fluid without the compressional relaxation process.

interaction of vibrating spheres in Maxwell fluids. This should be very useful to interpret the experimental measurements of vibrational dynamics of spheres.

- The eigenfrequency equation (18) can highlight that the combined effects of fluid compressibility and viscoelasticity can strongly affect the dynamics of spheres embedded in Maxwell fluids.

- The vibrational dynamics of nanospheres in compressible and incompressible viscoelastic fluids can changes dramatically, and this can be due to the effects of compressional and shear elasticity.

- The proposed model highlights by solving analytically the fluid-structure interaction of an elastic sphere executing spheroidal vibrations in fluid, the importance of combined effects of fluid compressibility and viscoelasticity on nanoscale flows.

- A significant reduction in the quality factor due to the fluid viscosity when water is replaced by water-glycerol mixture is observed for the spheroidal modes.

- A sensitivity of the breathing mode to the compressional relaxation process is also highlighted. However, the dipolar and quadrupolar modes are not affected by this compressional relaxation process. Therefore, to reasonably predict the quality factor, the compressional relaxation effect should be considered for the breathing mode. In other words, the Maxwell fluid with compressional relaxation process is more appropriate for breathing mode and, the Maxwell fluid without compressional relaxation process is more suitable for dipolar and quadrupolar modes.

- For low mass fractions, the compressional relaxation effect on the higher-order modes is less significant.

A. Appendix

Matrix elements given in Eq. (18) :

$$S_{11} = nJ_{n+\frac{1}{2}}\left(k_c a\right) - k_c a J_{n+\frac{3}{2}}\left(k_c a\right)$$

$$S_{12} = nY_{n+\frac{1}{2}}\left(k_c a\right) - k_c a Y_{n+\frac{3}{2}}\left(k_c a\right)$$

$$S_{13} = n(n+1)I_{n+\frac{1}{2}}\left(k_s a\right)$$

$$S_{14} = n(n+1)K_{n+\frac{1}{2}}\left(k_s a\right)$$

$$S_{15} = nJ_{n+\frac{1}{2}}\left(K_c a\right) - K_c a J_{n+\frac{3}{2}}\left(K_c a\right)$$

$$S_{16} = n(n+1)J_{n+\frac{1}{2}}\left(K_s a\right)$$

$$S_{21} = nJ_{n+\frac{1}{2}}\left(k_c a\right)$$

$$S_{22} = nY_{n+\frac{1}{2}}\left(k_c a\right)$$

$$S_{23} = k_s a I_{n-\frac{1}{2}}\left(k_s a\right) - nI_{n+\frac{1}{2}}\left(k_s a\right)$$

$$S_{24} = -k_s a K_{n-\frac{1}{2}}\left(k_s a\right) - nK_{n+\frac{1}{2}}\left(k_s a\right)$$

$$S_{25} = nJ_{n+\frac{1}{2}}\left(K_c a\right)$$

$$S_{26} = K_s a J_{n-\frac{1}{2}}\left(K_s a\right) - nJ_{n+\frac{1}{2}}\left(K_s a\right)$$

$$S_{31} = 2k_c a J_{n-\frac{1}{2}}\left(k_c a\right) - g\left(k_c^2\right)J_{n+\frac{1}{2}}\left(k_c a\right)$$

$$S_{32} = 2k_c a Y_{n-\frac{1}{2}}\left(k_c a\right) - g\left(k_c^2\right)Y_{n+\frac{1}{2}}\left(k_c a\right)$$

$$S_{33} = n(n+1)\left[(n+2)I_{n+\frac{1}{2}}\left(k_s a\right) - k_s a I_{n-\frac{1}{2}}\left(k_s a\right)\right]$$

$$S_{34} = n(n+1)\left[(n+2)K_{n+\frac{1}{2}}\left(k_s a\right) + k_s a K_{n-\frac{1}{2}}\left(k_s a\right)\right]$$

$$S_{35} = 2K_c a J_{n-\frac{1}{2}}\left(K_c a\right) - g\left(-K_s^2\right)J_{n+\frac{1}{2}}\left(K_c a\right)$$

$$S_{36} = n(n+1)\left[(n+2)J_{n+\frac{1}{2}}\left(K_s a\right) - K_s a J_{n-\frac{1}{2}}\left(K_s a\right)\right]$$

$$S_{41} = (n+2) J_{n+\frac{1}{2}}\left(k_c a\right) - k_c a J_{n-\frac{1}{2}}\left(k_c a\right)$$

$$S_{42} = (n+2) Y_{n+\frac{1}{2}}\left(k_c a\right) - k_c a Y_{n-\frac{1}{2}}\left(k_c a\right)$$

$$S_{43} = k_s a I_{n-\frac{1}{2}}\left(k_s a\right) - f\left(k_s^2\right)$$

$$S_{44} = -k_s a K_{n-\frac{1}{2}}\left(k_s a\right) - f\left(k_s^2\right)$$

$$S_{45} = (n+2) J_{n+\frac{1}{2}}\left(K_c a\right) - K_c a J_{n-\frac{1}{2}}\left(K_c a\right)$$

$$S_{46} = K_s a J_{n-\frac{1}{2}}\left(K_s a\right) - f\left(-K_s^2\right)$$

$$S_{51} = n J_{n+\frac{1}{2}}\left(k_c b\right) - k_c b J_{n+\frac{3}{2}}\left(k_c b\right)$$

$$S_{52} = n Y_{n+\frac{1}{2}}\left(k_c b\right) - k_c b Y_{n+\frac{3}{2}}\left(k_c b\right)$$

$$S_{53} = n(n+1) I_{n+\frac{1}{2}}\left(k_s b\right)$$

$$S_{54} = n(n+1) K_{n+\frac{1}{2}}\left(k_s b\right)$$

$$S_{61} = n J_{n+\frac{1}{2}}\left(k_c b\right)$$

$$S_{62} = n Y_{n+\frac{1}{2}}\left(k_c b\right)$$

$$S_{63} = k_s b I_{n-\frac{1}{2}}\left(k_s b\right) - n I_{n+\frac{1}{2}}\left(k_s b\right)$$

$$S_{64} = -k_s b K_{n-\frac{1}{2}}\left(k_s b\right) - n K_{n+\frac{1}{2}}\left(k_s b\right)$$

where

$$f\left(k^2\right) = n^2 + 2n + \frac{k^2 a^2}{2}$$

$$g\left(k^2\right) = n^2 + 3n + 2 - \frac{k^2 a^2}{2}$$

Breathing mode vibration :

For a breathing mode vibration, the nonzero component of displacement can be denoted $u_r = u_r(r,t)$. In this case the angular dependence of the breathing mode is equal to zero ($n = 0$), and the incompressible part of the velocity field (and displacement field) are equal to zero (i.e. $\psi = \Psi = 0$). Therefore, the scalar potentials, velocity, displacement and stress tensor components become :

$$\phi = A_1 \frac{e^{jk_c r}}{r}$$

$$v_r = A_1 \left(jk_c - \frac{1}{r}\right) \frac{e^{jk_c r}}{r}$$

$$T_{rr}^{(f)} = A_1 \left(\frac{4\eta^*}{r^2} - \frac{4j\eta^* k_c}{r} - j\omega \rho_f\right) \frac{e^{jk_c r}}{r}$$

$$\Phi = A_3 \frac{\sin\left(K_c r\right)}{r}$$

$$u_r = A_3 \left[\frac{K_c \cos\left(K_c r\right)}{r} - \frac{\sin\left(K_c r\right)}{r^2}\right]$$

$$T_{rr}^{(s)} = A_3 \left\{\frac{4\mu}{r}\left[\frac{\sin\left(K_c r\right)}{r^2} - \frac{K_c \cos\left(K_c r\right)}{r}\right]\right.$$

$$\left. - \frac{\lambda + 2\mu}{r} K_c^2 \sin\left(K_c r\right)\right\}$$

Hence, the matrix **S** given in Eq. (18) takes the following form

$$\mathbf{S} = \begin{pmatrix} v_r & j\omega u_r \\ T_{rr}^{(f)} & -T_{rr}^{(s)} \end{pmatrix}_{r=a}$$

It can be shown, after some manipulation, that the determinant of this 2×2 matrix is given in Eq. (19).
To obtain Eq. (20), k_c must be replaced by k_c^* in Eq. (19) .

References

[1] S. S. Verbridge, L. M. Bellan, J. M. Parpia and H. G. Craighead. Optically driven resonance of nanoscale flexural oscillators in liquid, *Nano Lett.* **6** (9), 2109–2114 (2006).

[2] H. Portales, N. Goubet, L. Saviot, S. Adichtchev, D. B. Murray, A. Mermet, E. Duval and M. P. Pileni. Probing atomic ordering and multiple twinning in metal nanocrystals through their vibrations, *Proc. Natl. Acad. Sci.* **105**(39), 14784–14789 (2008).

[3] K. Jensen, K. Kim and A. Zettl. An atomic-resolution nanomechanical mass sensor, *Nat. Nanotechnol.* **3**, 533–537 (2008).

[4] J. L. Arlett, E. B. Myers and M. L. Roukes. Comparative advantages of mechanical biosensors, *Nat. Nanotechnol.* **6**, 203–215 (2011).

[5] P. V. Ruijgrok, P. Zijlstra, A. L. Tchebotareva, M. Orrit. Damping of Acoustic Vibrations of Single Gold Nanoparticles Optically Trapped in Water, *Nano Lett.* **12**(2), 1063–1069 (2012).

[6] D. Chakraborty, E. V. Leeuwen, M. Pelton and J. E. Sader. Vibration of nanoparticles in viscous fluids, *J. Phys. Chem. C* **117**(16), 8536–8544 (2013).

[7] M. Babincova, P. Sourivong and P. Babinec. Resonant absorption of ultrasound energy as a method of HIV destruction, *Med. Hypotheses* **55**(5), 450–451 (2000).

[8] L. H. Ford. Estimate of the vibrational frequencies of spherical virus particles, *Phys. Rev. E* **67**, 051924 (2003).

[9] L. Saviot, D. B. Murray, A. Mermet, and E. Duval. Comment on estimate of the vibrational frequencies of spherical virus particles, Phys. Rev. E **69**, 023901 (2004).

[10] M. Talati and P. K. Jha. Acoustic phonon quantization and low-frequency Raman spectra of spherical viruses, *Phys. Rev. E* **73**, 011901 (2006).

[11] S. Sirotkin, A. Mermet, M. Bergoin, V. Ward, J. L. Van Etten. Viruses as nanoparticles: Structure versus collective dynamics, *Phys. Rev. E* **90**, 022718 (2014).

[12] G. V. Hartland. Coherent excitation of vibrational modes in metallic nanoparticles, Annu. Rev. Phys. Chem. **57**, 403–430 (2006).

[13] M. Fujii, T. Nagareda, S. Hayashi, S. Hayashi and K Yamamoto. Low-frequency Raman scattering from small silver particles embedded in SiO2 thin films, *Phys. Rev. B* **44**(12), 6243–6248 (1991).

[14] H. Lamb. On the vibrations of an elastic sphere, *P. Lond. Math. Soc.* **13**, 189–212 (1882).

[15] V. A. Dubrovskiy and V. S. Morochnik. Natural vibrations of a spherical inhomogeneity in an elastic medium, *Phys. Solid Earth* **17**(7), 494–504 (1981).

[16] D. E. Kheisin. Radial oscillations of an elastic sphere in a compressible fluid, *Fluid Dyn.* **2**, 53–55 (1967).

[17] D. L. Jain, R. P. Kanwal. Scattering of elastic waves by an elastic sphere, *Int. J. Eng. Sci.* **18**(9), 1117–1127 (1980).

[18] E. Duval, A. Boukenter, and B. Champagnon. Vibration Eigenmodes and Size of Microcrystallites in Glass: Observation by Very-Low-Frequency Raman Scattering, Phys. Rev. Lett. **56**, 2052 (1986).

[19] E. Duval. Far-infrared and Raman vibrational transitions of a solid sphere: Selection rules., Phys. Rev. B **46**(9) (1992).

[20] S. V. Goupalov, L. Saviot and E. Duval. Comment on Infrared and Raman selection rules for elastic vibrations of spherical nanoparticles, Phys. Rev. B **74**, 197401 (2006).

[21] G. Bachelier, J. Margueritat, A. Mlayah, J. Gonzalo, and C. N. Afonso. Size dispersion effects on the low-frequency Raman scattering of quasispherical silver nanoparticles: Experiment and theory, Phys. Rev. B **76**, 235419 (2007).

[22] S. Reymond-Laruinaz, L. Saviot, V. Potin, C. Lopes, F. Vaz and M. C. Marco de Lucas. Growth and size distribution of Au nanoparticles in annealed Au/TiO2 thin films, Thin Solid Films **553**(28), 138–143 (2014).

[23] B. Stephanidis, S. Adichtchev, P. Gouet, A. McPherson and A. Mermet. Elastic Properties of Viruses, *Biophys. J.* **93**(4), 1354–1359 (2007).

[24] T. M. Liu, H. P Chen, L. T. Wang, J. R Wang, T. N. Luo, Y. J. Chen, S. I Liu, and C. K Sun. Microwave resonant absorption of viruses through dipolar coupling with confined acoustic vibrations, Appl. Phys. Lett. **94**, 043902 (2009).

[25] S. C. Yang, H. C. Lin, T. M. Liu, J. T Lu, W. T. Hung, Y. R. Huang, Y. C. Tsai, C. L. Kao, S. Y. Chen and C. K. Sun. Efficient Structure Resonance Energy Transfer from Microwaves to Confined Acoustic Vibrations in Viruses, Sci. Rep. **5**, 18030 (2015).

[26] V. Galstyan, O. S. Pak and H. A. Stone. A note on the breathing mode of an elastic sphere in Newtonian and complex fluids, *Phys. Fluids* **27**, 032001 (2015).

[27] D. Chakraborty and E. Sader. Constitutive models for linear compressible viscoelastic flows of simple liquids at nanometer length scales, Phys. Fluids **27**, 052002 (2015).

[28] D. D. Joseph. Fluid Dynamics of viscoelastic liquids, Springer (1990).

[29] T. Jongen, T. B. Gatski. Tensor representations and solutions of constitutive equations for viscoelastic fluids, *Int. J. Eng. Sci.* **43**, 556–588 (2005).

[30] L. D. Landau and E. M. Lifshitz. Fluid Mechanics (Pergamon, Oxford) (1959).

[31] P. M. Morse and H. Feshbach. Methods of theoretical physics Part II. (McGraw-Hill, New York, 1946).

[32] M. Hu, X. Wang, G. V. Hartland, P. Mulvaney, J. P. Juste, and J. E. Sader. Vibrational response of nanorods to ultrafast laser induced heating: Theoretical and experimental analysis, *J. Am. Chem. Soc.* **125**, 14925-14933 (2003).

[33] M. Pelton, D. Chakraborty, E. Malachosky, P. Guyot-Sionnest and J. E. Sader. Viscoelastic Flows in Simple Liquids Generated by Vibrating Nanostructures, *Phys. Rev. Lett.* **111**(24), 244502 (2013).

[34] M. Pelton, J. E. Sader, J. Burgin, M. Z. Liu, P. Guyot-Sionnest, and D. Gosztola, Damping of acoustic vibrations in gold nanoparticles, *Nat. Nanotechnol.* **4**, 492–495 (2009).

[35] T. A. Major, A. Crut, B. Gao, S. S. Lo, N. D. Fatti, F. Vallee, and G. V. Hartland, Damping of the acoustic vibrations of a suspended gold nanowire in air and water environments, *Phys. Chem. Chem. Phys.* **15**(12), 4169-4176 (2013).

[36] L. Saviot, D. B. Murray, A. Mermet, and E. Duval. Damping by Bulk and Shear Viscosity of Confined Acoustic Phonons for Nanostructures in Aqueous Solution, *J. Phys. Chem. B* **111**(25), 7457–7461 (2007).

[37] V. Juvé, A. Crut, P. Maioli, M. Pellarin, M. Broyer, N. Del Fatti and F. Vallée. Probing Elasticity at the Nanoscale: Terahertz Acoustic Vibration of Small Metal Nanoparticles, *Nano Lett.* **10**(5), 1853–1858 (2010).